Kabli, Mohammad R.; Ali, Arshid M.; Inayat, Muddasser; Zahrani, Abdulrahim A.; Shahzad, Khurram; Shahbaz, Muhammad; Sulaiman, Shaharin A.

H_2-rich syngas production from air gasification of date palm waste : an experimental and modeling investigation

Published in:
Biomass Conversion and Biorefinery

DOI:
10.1007/s13399-022-02375-7

E-pub ahead of print: 10/02/2022

Document Version
Peer-reviewed accepted author manuscript, also known as Final accepted manuscript or Post-print

Please cite the original version:
Kabli, M. R., Ali, A. M., Inayat, M., Zahrani, A. A., Shahzad, K., Shahbaz, M., & Sulaiman, S. A. (2022). H_2-rich syngas production from air gasification of date palm waste : an experimental and modeling investigation. *Biomass Conversion and Biorefinery*. Advance online publication. https://doi.org/10.1007/s13399-022-02375-7

H_2-rich syngas production from air gasification of date palm waste: An experimental and modeling investigation

Mohammad R. Kabli[1], Arshid M. Ali[2*], Muddasser Inayat[3,4], Abdulrahim A. Zahrani[2], Khurram Shahzad[5], Muhammad Shahbaz[6], Shaharin A. Sulaiman[3]

[1]Department of Industrial Engineering, Faculty of Engineering, King Abdulaziz University, Jeddah, Saudi Arabia.

[2]Department of Chemical and Materials Engineering, Faculty of Engineering, King Abdulaziz University, Jeddah, Kingdom of Saudi Arabia.

[3]Department of Mechanical Engineering, Universiti Teknologi PETRONAS, 32610 Seri Iskandar, Perak Darul Ridzuan, Malaysia.

[4]Research Group of Energy Conversion, Department of Mechanical Engineering, School of Engineering, Aalto University, 02150 Espoo, Finland.

[5]Center of Excellence in Environmental Studies (CEES), King Abdulaziz University, Jeddah, Kingdom of Saudi Arabia.

[6]Division of Sustainable Development, College of Science and Engineering, Hamad Bin Khalifa University, Qatar Foundation, Education City, P.O. Box 5825, Doha, Qatar.

Corresponding author: amsali@kau.edu.sa

Abstract:

The energy generation from renewable sources is in prime focus not only oil-importing countries as well as oil-exporting countries. This study aims to probe out the energy generation (syngas) from Saudi Arabian date palm fronds through air gasification in a downdraft fixed bed system. In addition, an equilibrium process simulation model was developed using Aspen Plus and predicted results were compared with experimental results. Furthermore, mass and energy flows of the system were also analyzed. In parametric study, the impact of temperature (600-900°C), particle size (2-6 mm) and air flowrate (1-4 l/min) were investigated on syngas composition and gasification performance parameters higher heating value, gas yield, carbon conversion efficiency, and cold gas efficiency. The results indicate that H_2 concentration was enhanced with the rise of temperature and particle size from 12.12 to 26 vol.% and 26.02 to 26.89 vol.% respectively. The enrichment of H_2 concentration was due to the activation of endothermic reaction and methane reforming reaction as CH_4 was dropped with increased temperature. The higher heating value of syngas, carbon conversion efficiency, and cold gas efficiency have shown an increasing profile with increased in temperature and air flowrate. The gas concentration profile obtained from the simulation model found good agreement with the experimental results. The energy analysis shows that the process is highly energy consuming, and most of the energy waste is in the form of condensate that could be potentially utilized. This study will be helpful for researchers and commercial enterprises to produce syngas from Saudi Arabian date palm fronds.

Keywords: Date palm fronds, Syngas composition, Aspen Plus simulation, Mass & energy flow, Gasification.

Highlights:

- Date palm fronds (DPF) gasification was performed in downdraft fixed bed gasifier.

- Temperature, particle size, air flowrate impact was investigated on gas composition.
- Equilibrium simulation model was developed in Aspen Plus for DPF air gasification.
- Impact of temperature, particle size, air flowrate was analyzed on gasification performance.
- Mass and energy flows were analyzed to find heat requirement of process.

1. Introduction

Energy is considered an essential need of modern human living, and all nodes of modern life are based on the continuous supply of energy [1]. Many developed countries consume ample quantity of energy to sustain their industrial and economic activities [2]. Fossil fuel is still the backbone of world energy supply by providing the 80% share of world energy generation, which is gobbling the fossil sources. Excessive use of fossil fuels contributes to a negative impact on the environment, causing the emission of greenhouse gases, which eventually increases the 2℃ average global temperature and a serious threat to the world future which is indicated in Intergovernmental Panel on Climate Change [3,4]. The world leaders agreed in the Paris climate change conference to shift energy generation toward renewable energy resources to combat climate change [2]. In this context, agriculture and forest (biomass) emerge as potential renewable energy resources, especially to produce gaseous fuel via the gasification process [5]. Gasification is a thermochemical conversion approach that converts the low-cost waste solid fuel into valuable gas phase fuel at elevated temperatures of 600℃ to 1000℃ in the presence of oxidizing agent known as a gasification medium [6,7]. Gasification has many advantages over simple combustion as it produces low CO_2 emission and negative CO_2 emission using CO_2 capturing methods [2]. The main gasification product is gas, which includes mainly H_2, CO, CH_4, CO_2, and some liquid hydrocarbons.

Kingdom of Saudi Arabia (KSA) is the largest and an important country in the Gulf region. It has copious resources of crude oil and natural gas [8]. The standard of life in KSA is continuously improving. As a result, the consumption of electricity per capita is also increasing, which is one of the high in the world. KSA power generation sector is highly dependent on crude oil and natural gas. KSA is known for its date fruits; a significant growth in date fruits has been noticed over the last two decades, matched by increasing demand [9]. KSA is one of the largest producers of dates fruits globally, accounting for 17% of worldwide supply. According to an estimation, about 31 million date palm trees are in KAS and produce over 1.5-million-ton date fruits each year. In addition, KSA exports about 222 thousand tons of dates in 2021 which is about 12% of the world supply having a worth of SAR 1.75 billion [10]. Along with the date fruits, the date palm field has a lot of biomass wastes; according to an estimate, almost 20 kg of waste leave and fronds are produced from a single date palm tree in a year. Besides these wastes, it also produces date pits, which account for 10% of the date fruits weight [11].

KSA is heavily dependent on fossil fuels for its energy needs. Now KSA is transforming its energy generation toward renewable energy, which is more environmental friendly. Therefore, in this context, energy extraction from biomass emerged as a potential and doable energy source. KSA date palm fields produce abounded quantity of date palm wastes, and these wastes

are underutilized. The renewable energy advancement in oil-exporting nations like KSA is slower than in oil-importing countries is due to abundant, low-cost fossil fuel and limited renewable energy supplies. Vision 2030, in which Renewable and Sustainable Energy project is a significant revolution for the renewable energy scenario in Saudi Arabia, intending to run NEOM city entirely on renewable energy [12].

Considering the above scenario, using date palm waste for energy generation will be a viable option. With this abundance of date palm trash in oil-rich nations and energy extraction from this abundant date palm waste has not received much attention in KSA due to ample sources of crude oil [13]. However, the energy excretion from date seeds has been increased using the pyrolysis process for char and bio-oil. Bensidhom *et al*. 2018 [14] used Tunisian date palm wastes for the pyrolysis process in a fixed bed reactor, yielding 31.66% char and 17.99% bio-oil, respectively. Whereas Sait *et al*. 2018 [15] performed the kinetics of date palm waste for combustion and pyrolysis process using a thermogravimetric analyzer to determine the combustion and pyrolysis process properties. Later, microwave pyrolysis of date palms was found very effective for char production [16].

Although the date palm is mostly utilized for pyrolysis, date palm gasification has received little attention. Bassyouni *et al*. 2014 [17] employed Aspen Plus to configurated a date palm steam-gasification process and predict the enhancement of H_2 generation by 50% to 56% with the increase of steam flowrate. Later AlNouss *et al*. 2018 [19] also instituted a simulation model and used the thermo-equilibrium method to co-gasify Qatarin date pits, manure, and sludge, and predicted syngas yields of 1.96-2.27/$kg_{feedstock}$. Sulaiman *et al*. 2020 [24] reported the energy conversion potential of three date palm fronds of Ajwah, Sukariah, and Jeddah date palm by using thermochemical characteristics. Characterizations included ultimate and proximate analysis, heating value, SEM with EDX based elemental analysis and results were compared with other conventional biomasses. The effect of temperature and particle size on gas composition and heating value was also investigated [24]. Martis *et al*. 2020 [18] developed a simulation model for pyrolysis, gasification, and combustion of date palm waste for energy generation and also performed a techno-economic analysis for commercial viability. It is clear from literature survey that experimental work reported on date palm fronds (DPF) gasification is limited focus. The gas composition, yield, and heating content of syngas produced are influenced by process parameters like temperature, gasification agent, and feedstock particle size. [20,3]. The temperature has a paramount role in the gasification process. It directly influences methane reforming, water gas shift, and Boudouard reactions, which directly impact the composition of gases and products output [21]. The influence of the gasification agent is directly related to the gas composition and yield. Steam is better for enriching hydrogen and composition than air because it stimulates the water gas shift reaction. Air is less expensive compared to steam and produces a decent amount of H_2 in the product gas. The gas yield, carbon conversion efficiency, and cold gas efficiency are directly influenced by the air flowrate and quantity of air [22]. The particle size (d_p) of the feedstock is important in heat and mass transfer properties since it directly affects material thermal decomposition into gas, liquid, and char [23].

It is clear from the above discussion that there are very few studies documented to produce syngas from DPF. The conversion of DPF into syngas through the gasification process and the performance of the gasification systems have not been documented. The study aims to perform the air gasification of DPF in a downdraft fixed bed to investigate the gas production potential in KSA. A process simulation model for air gasification was also developed for detailed investigation by employing Aspen Plus. The first objective is to examine the impact of three operating parameters temperature (600-900°C), air flowrate (1-4 l/min), and particle size (d_p of 2-6 mm) on gas composition and gasification performance parameters such as CCE, syngas higher heating value (HHV), CGE, and gas yield. The second objective is to configure a process simulation model using Aspen Plus in the same operating conditions used in the experimental setup. The gas product obtained from the simulation is compared with experimental gas composition performed at lab scale downdraft gasifier. The energy analysis is carried out to understand the energy requirement and energy generation to identify commercial viability of process.

2. Feedstock and Methodology

2.1. Feedstock preparation and characterization

Air-dried DPF without leaflets of Mishriq date palm variety were received from the KSA. The DPF feedstock was prepared for the characterization. The DPF was ground using a mechanical granulator and screened to a particle size of 250 µm in sieve shaker for characterization. The characterization of DPF consists of three important tests to assess its properties as fuel such as ultimate analysis, proximate analysis, and calorific value analysis. The physical and chemical properties of DPF are presented in Figure 1 and Table 1. The DPF feedstock was prepared for gasification experiments in a mechanical granulator and sieved to particle size (d_p) of >6, 6-2, 2, and <2 mm as shown in Figure 1.

Figure 1. Prepared date palm fronds feedstock at various particle size (d_p) for air gasification.

Table 1: Chemical properties of date palm fronds (DPF)

Feedstock	Ultimate analysis (wt.% dry basis)					Proximate analysis (wt.% dry basis)			HHV MJ/kg
	C	H	N	S	O	Volatile matter	Fixed Carbon	Ash	
DPF	36.58	5.85	3.15	0.28	54.13	80.35	12.66	6.99	16.62

2.2. Gasification operation

Gasification process was performed at a bench-scale downdraft gasifier system as shown in Figure 2. An external jacketed heater was used to heat up the gasifier at the desired temperature. The gasifier, its related equipment, connected pipelines, and hoses were cleanup for any dirt of ash, char, and excretion of the previous experiment. The temperature inside the gasifier was gauged and controlled with a thermocouple and electric microcontroller respectively. The range of temperature selected for the current investigation was varied from 600°C to 900°C. The gasifier turned on to heat up to the target temperature through electric heating coils embedded in ceramic materials. The 100 g of DPF (particle size, d_p varied from <2 mm to >6 mm) was fed into the gasifier after heating the gasifier at augmented temperature. According to the designed air flowrate (1-4 l/min), the air was poured into the gasifier to oxidize the feedstock. The produced syngas pass through the gas filter, gas cooling system, and ceramic filter to clean and cooled down the gas and removed dust and traces of soot from the gas. The clean and cooled down syngas was analyzed by Emerson X-stream online gas analyzer to quantify the product of syngas composition. This online gas analyzer was annexed with a computer to record the gas concentrations with an interval of one second. The remaining syngas was burnt at a flare point in a gas burner as show in Figure 2.

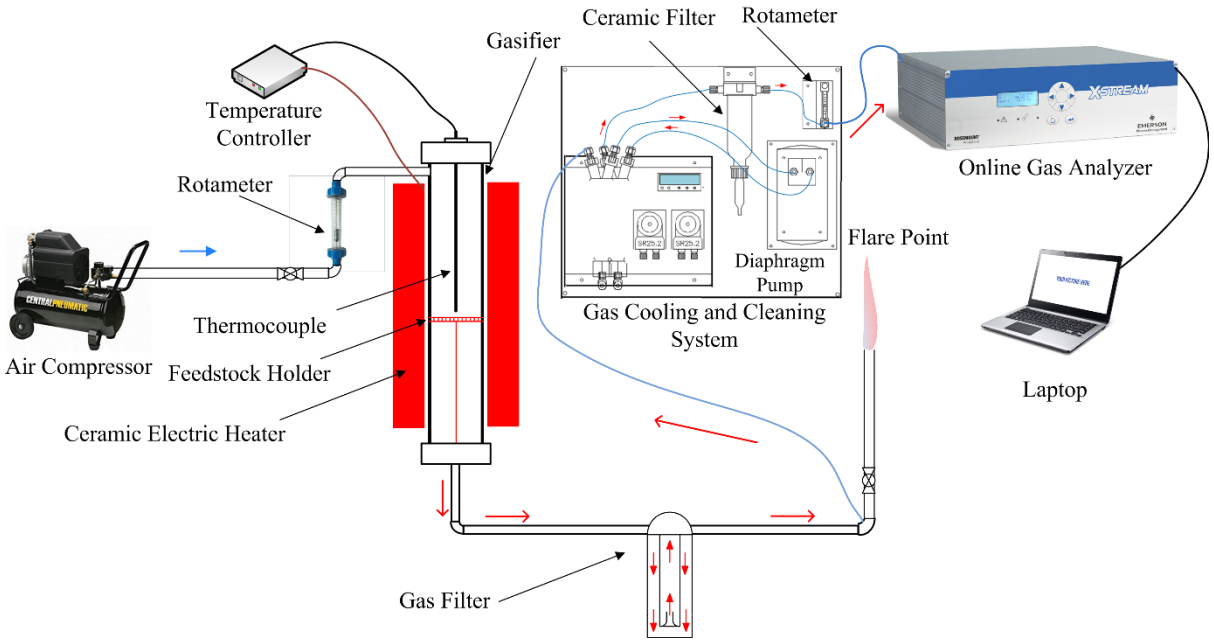

Figure 2. Schematic diagram of air gasification set-up.

2.3. Gasification performance

The system performance was measured in terms syngas higher heating value (HHV) MJ/Nm^3 [25], and gas yield (Y) Nm^3/kg [25,26]. The system efficiency evaluated as the cold gas efficiency (CGE) and carbon conversion efficiency (CCE) [27,28]. HHV of syngas was calculated by Eq.1, whereas X_{CO}, X_{H_2}, and X_{CH_4} presents the fraction proportion of respected gas in syngas respectively.

$$HHV_{syngas}=12.63\times X_{CO}+12.74\times X_{H_2}+39.82\times X_{CH_4} \quad (1)$$

Gas yield was determined using Eq. 2, whereas Y, Q_a, W_b, X_{ash}, and N_2 denotes gas yield, air flowrate (Nm^3/h), mass flowrate of DPF (kg/h), fraction of ash in DPF, percentage of nitrogen fraction in the syngas respectively.

$$Y = \frac{Q_a \times 79\%}{W_b(1 - X_{ash})N_2\%} \text{ Nm}^3/\text{kg} \quad (2)$$

Cold gas efficiency (η_{th}) was measured by Eq. 3, whereas H_g, H_b, and Y presents HHV_{syngas}, HHV_{DPF}, and gas yield respectively.

$$\eta_{th} = \frac{H_g(\text{MJ/Nm}^3) \times Y(\text{Nm}^3/\text{kg})}{H_b(\text{MJ/kg})} \times 100\% \quad (3)$$

Carbon conversion efficiency (η_c) of gasification was determined using Eq. 4, whereas Y, M_C, and C% presents gas yield, atomic mass of carbon, and carbon content of DPF. Whereas CO%, CO_2%, and CH_4% denotes volumetric% of gas fraction in syngas.

$$\eta_c = \frac{Y(CO\% + CO_2\% + CH_4\%) \times M_C}{22.4 \times C\%} \times 100\% \quad (4)$$

2.4. Process simulation approach

The process simulation model was developed for the gasifier model using a computer-aided technique Aspen Plus. It is an effective and high-performance simulation software used extensively in chemical engineering research and commercial process development. The experimental setup was simulated in Aspen Plus, and the predicted results were compared with experimental data. Some critical assumptions were considered for the smooth simulation process. The process is developed at a steady state in zero-dimension conditions. Isothermal conditions and atmospheric pressure were maintained for process propagation. The other vital assumptions were considered, such as no pressure gradient, char was taken 100% of carbon, and tar formation neglected. The elements like S, N_2, and Cl were converted into hydrogen sulphide, ammonia, and hydrochloric acid [29].

The process flowsheet was developed as shown in Figure 3. The MIXNCPSD stream class was chosen for simulation because solid biomass of DPF was treated as a non-conventional component. The Peng-Robison fluid package was selected used frequently for gas and petrochemical operations [29]. The feedstock stream of DPF was entered in to yield reactor (YIELDRT) to convert the non-conventional component into the conventional elements using calculator block given in Table 2 according to the mass composition set by proximate and ultimate analysis as presented in Table 1. The outlet stream from the YIELRCT was admitted to the GASIFR (an equilibrium reactor) operating at 750°C and 1 atm pressure. The AIR stream consists of required air added from the bottom as a gasifying agent. The gasification process was carried out in an equilibrium reactor on Gibbs free energy model, which allowed to propagate the reactions in phase equilibrium and chemical equilibrium mode to produce the gas. The ash was removed from the PRODGAS using a separate which was nomenclature as SEPRAT. The ash-free produced gas (PRODGAS stream) was passed through the condenser (COOLER) to cool down the gas for analysis. H_2 was separated from rest of gases using separator.

Table 2: Calculator block used for conversion of DPF into conventional element

Water = PROXANAL	(5)	N_2 = ULT(8)/100*((100-WATER)/100)	(10)
H_2O = WATER/100	(6)	Cl_2 = ULT(9)/100*((100-WATER)/100)	(11)
Ash = ULT(5)/100*((100-WATER)/100)	(7)	Sulfur = ULT (10)/100*((100-WATER)/100)	(12)
Carbon = ULT(6)/100*((100-WATER)/100)	(8)	O_2 = ULT (11)/100*((100-WATER)/100)	(13)
H_2 = ULT (7)/100*((100 WATER)/100)	(9)		

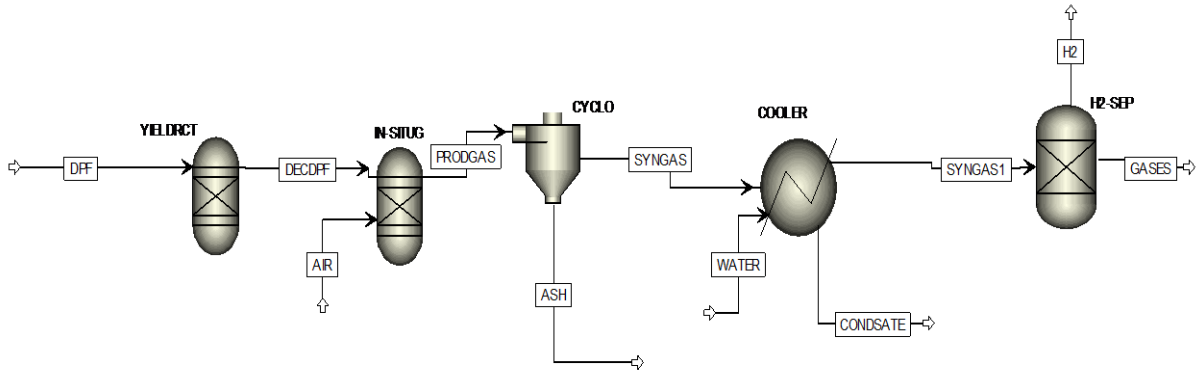

Figure 3. Process flowsheet diagram for date palm fronds air gasification.

3. Results and Discussion

3.1. Experimental results

3.1.1. Impact of temperature on gas composition and system performance

The temperature has a domino impact in the gasification process. The temperature has affected each reactions stage of the gasification process such as devolatilization, combustion, propagation of reaction, and reaction rate order. It does not only influence the product gas composition as well as the gasification performance such as syngas heating values, gas yield, CCE and CGE [3]. In this study, the impact of temperature from 600-900℃ is investigated at the air flowrate of 3.0 l/min. Figure 4a depicted the impact of temperature on the major component of product gas H_2, CO, CO_2, and CH_4 (free of N_2 and O_2). H_2 is a vital component of the product gas that is used as fuel and important for many chemicals manufacturing along with CO. The H_2 concentration increased in gas composition from 12.88 to 26.02 vol% in the range of 600-900℃. A similar increasing profile is observed for CO, which is the second most important component of syngas. The enrichment of both components in produced gas with the increasing temperature is due to the intensification of thermal cracking and methane-reforming reaction at elevated temperatures [30]. Contrarily, the composition of CH_4 and CO_2 has a decreasing trend with the increase of temperature is the result of the conversion of methane into H_2 and CO. The second important reaction is Boudouard, in which CO_2 convert into CO after reacting with carbon content of DPF. The looming of H_2 and CO and shrinkage of CH_4 and CO_2 with the temperature elevation due to the escalation of these reactions were also noticed in other studies [26,31,32].

In the case of gasification performance, an increase in HHV from 11.28 to 12.96 MJ/Nm^3 is noticed with the increase of temperature due to enrichment of H_2 and CO concentration as calculated by Eq. (1). Figure 4b shows that the CGE is also boosted with increased of

temperature and it is based on the HHV of product gas and feed. This increasing trend of HHV and CGE is the direct function of these gases in the product gas. CCE is in the range of 79-90% by elevating the temperature from 600 to 900℃. CCE is an estimate for the content of carbon-containing gases and carbon in feedstock. In this case, the net carbon content increases in product gas due to swapping carbon content of DPF by CO_2 and CH_4 to CO fractions. Similar profiling of gasification performance was also noticed by other researchers and documented [3,33].

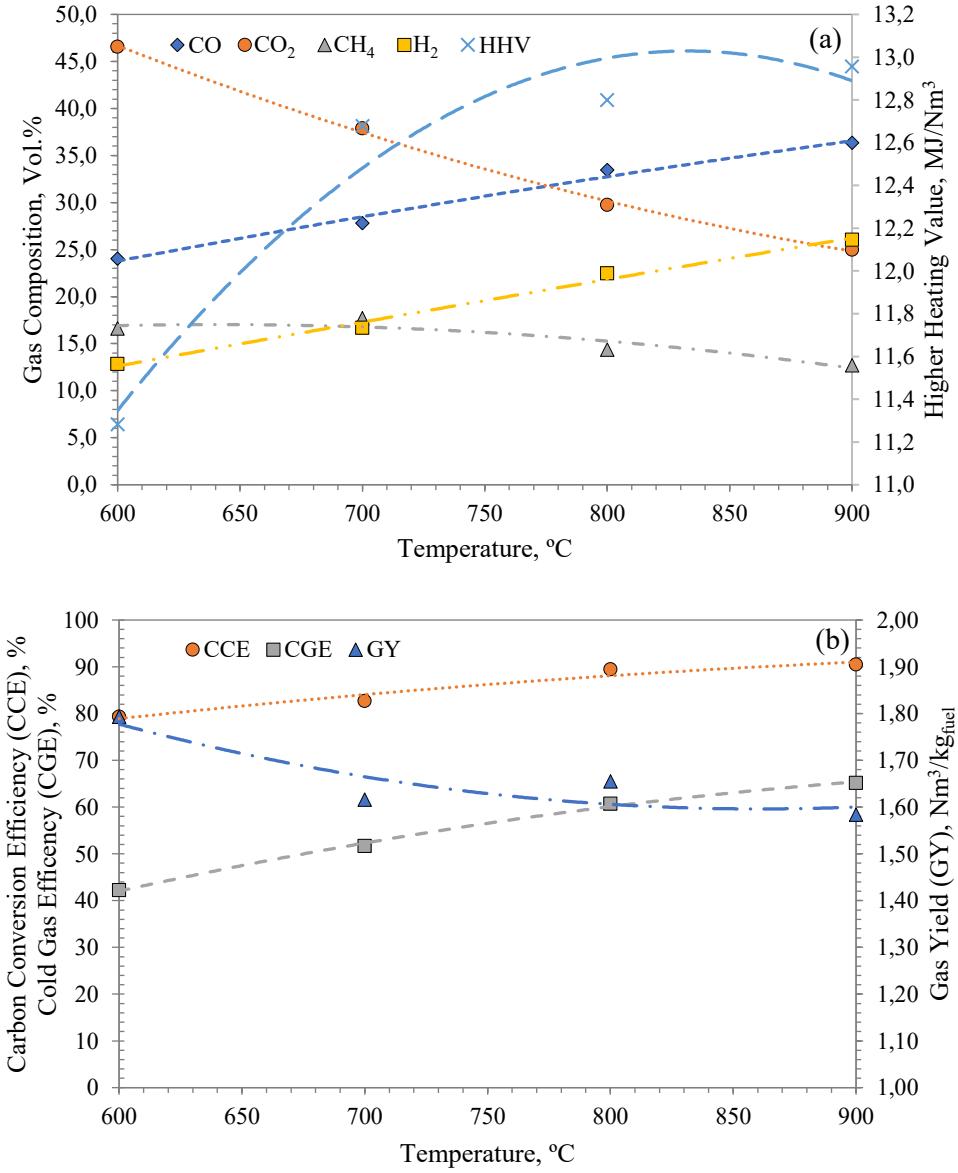

Figure 4. Impact of gasification temperature on (a) syngas composition and (b) gasification performance during the DPF gasification at air flowrate of 3.0 l/min and Particle size (d_p) 6-2 mm.

3.1.2. Impact of air flowrate on gas-composition and system performance

The air flowrate influences the gasification process and gas composition because air provides the oxygen to oxidize the DPF to convert into syngas using the gasification reactions. Figure 5a demonstrates the impact of air flowrate from 1-4 l/min on gas composition. H_2 and CO concentration is varied from 19.02 to 28.02 vol% and from 27 to 35 vol%, respectively. The maximum H_2 concentration of 28.27 vol% is noticed at air flowrate of 2.5 l/min and CO concentration 35 vol% at a higher air flowrate of 4.0 l/min. The enrichment in H_2 content is due to the activation of water gas shift reaction in the forward direction. A decreased in H_2 concentration was observed at higher flowrates probably due to formation of more CO and CO_2 fraction in the presence of excess of O_2 supply which reacts with carbon content of DPF. Whereas methane formation is decreased from 19.85 to 15.70 vol% with the increase of air flowrate is because of the methane reforming at system is occurring at higher temperature. The evidence of similar methane formation profiling was also recorded in previous studies [34]. The HHV of syngas follow the similar trend of H_2 concentration and maximum HHV of 14.60 MJ/Nm^3 at air flowrate of 2.5 l/min. This is due to higher H_2 and CH_4 concentration, which are main contributor of heating content according to Eq. 1. The CCE is increasing from 75.72 to 89.00 % with the addition of more air in the system as shown in Figure 5b. The increase of CCE is the direct function of carbon containing gases, and their concentration remains increases with the increase of air flowrate. In comparison, the CGE follows a similar trend of HHV as it determines based on HHV of gas and DPF. The same profiling of gasification performance was also reported in other studies [3,35].

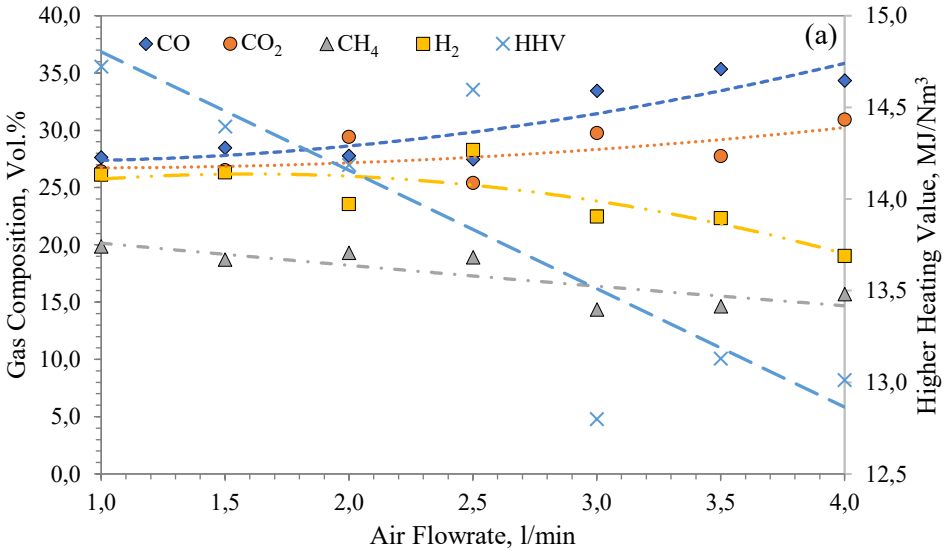

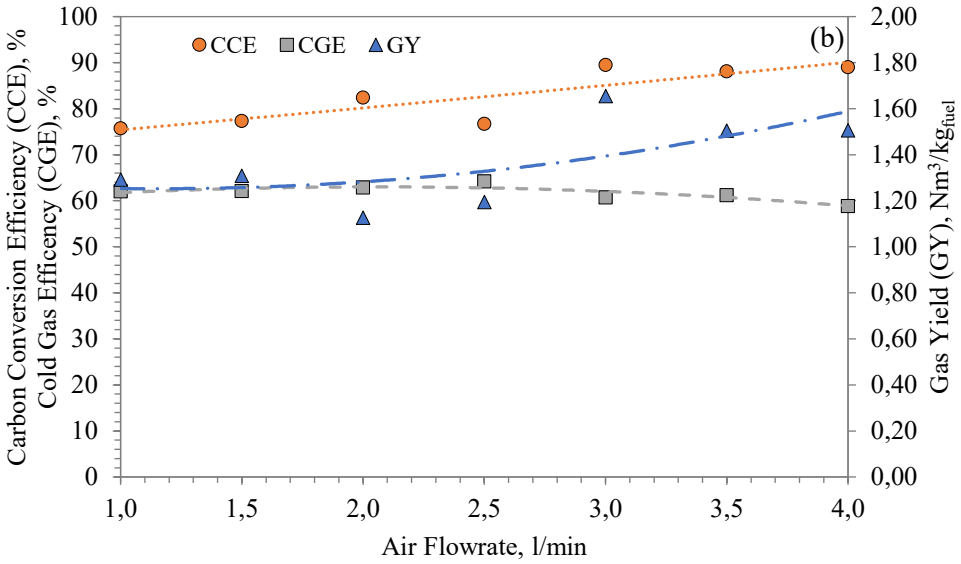

Figure 5. Impact of air flowrate on (a) syngas composition and (b) gasification performance during the DPF gasification at temperature of 800ºC and Particle size (d_p) 6-2 mm.

3.1.3. Impact of particle size on gas composition and system performance

Figure 6 depicts the impact of DPF particle size (d_p) on the concentration of gas and gasification performance. It can be noticed from Figure 6a, the H_2, CO and CH_4 concentrations are high at a moderate particle size of 4 mm. The increase in the concentrations of above mention gases at a bigger particle size and vice versa was also observed by other researchers [36]. The enrichment of higher yield of these gases is due to better heat flux and mass transfer due to the larger surface area available [37]. The lower formation of H_2 and CH_4 at a smaller feed particle size may be related to the lower diffusion rate of volatile products at the devolatilization phase [38]. HHV of product gas varied from 12.07 to 13.06 MJ/Nm^3 at different particle sizes. The slight variation in HHV is due to the slight variation in H_2, CO and CH_4, which is not more than 4 vol%. The CCE is reduced with the increase of particle size is due to the reduction of CO_2, CO, and CH_4 because CCE is the direct function of carbon-containing gases and carbon in feedstock. On the other hand, CGE is maximum at medium particle sizes of 2 and 4 mm as shown in Figure 6b. The CGE is directly related to the HHV and HHV is based on the composition of product gas [3].

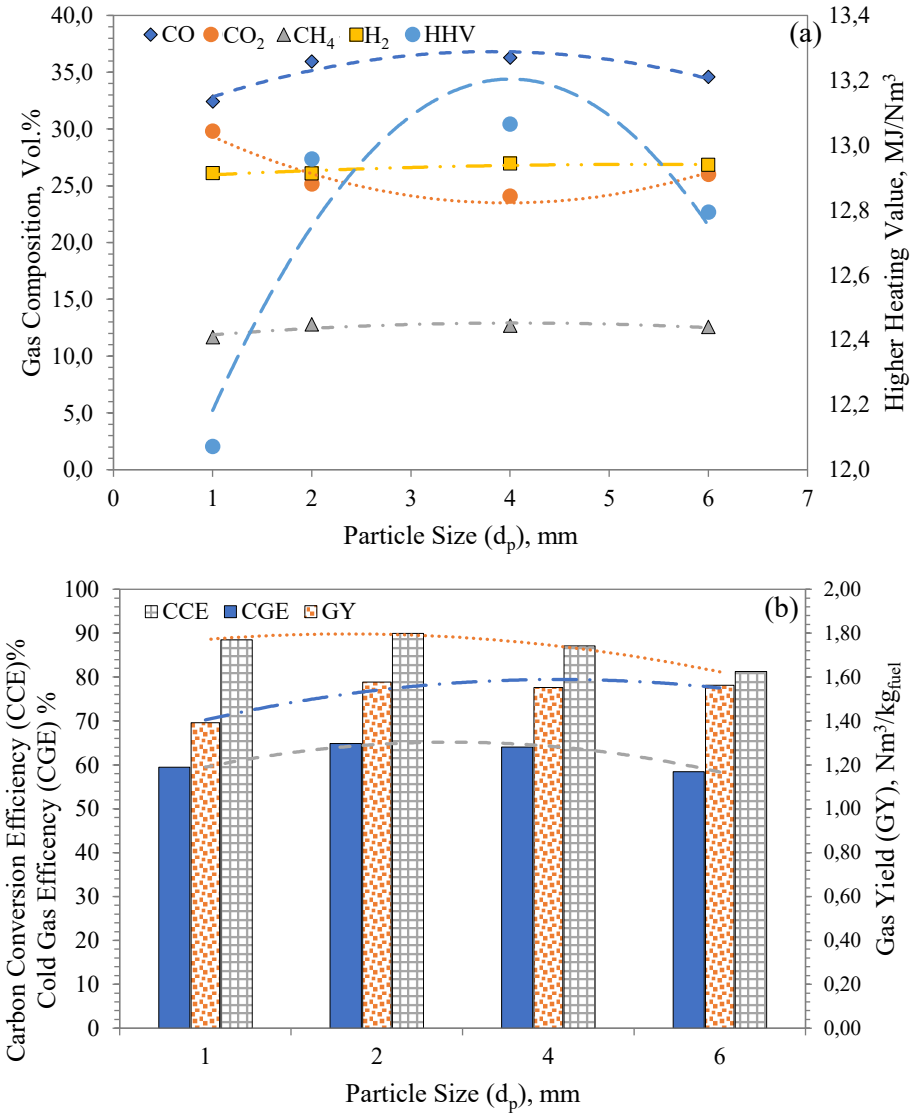

Figure 6. Impact of gasification particle size (d_p) on (a) syngas composition and (b) gasification performance during the DPF gasification at temperature of 900ºC and air flowrate 2.5 l/min.

3.2 Process simulation results

3.2.1. Impact of temperature on gas composition and syngas HHV

The process simulation model for DPF air gasification is predicted the gas composition. The impact of temperature on gas composition and syngas HHV is depicted in Figure 7a. The simulation results of gas concentration as given in Figure 7a shows a similar trend to experimental gas concentration obtained from DPF air gasification Figure 4a. Figure 7b presents the validation of simulation with experimental results at selected points. It is shown in Figure 7b that at 700°C temperature, experimental H_2, CO, and CO_2 concentrations are relatively less than predicted by simulation. Whereas methane concentration is about 9% higher in the experiment than in the modelling results. The difference in composition of other gases is due to the lower prediction of methane formation in the model. Whereas at the higher

temperature of 800 and 900℃, H_2, CO, and CO_2 production show similar composition trends just like experiments with less than 5% of deviation. Overall simulation gas concentrations were found to comparable trend with experimental gas concentrations.

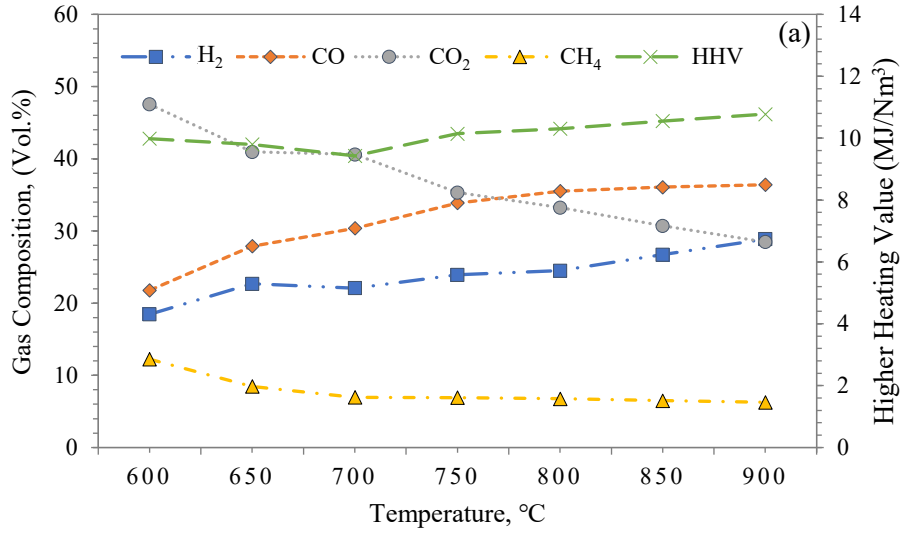

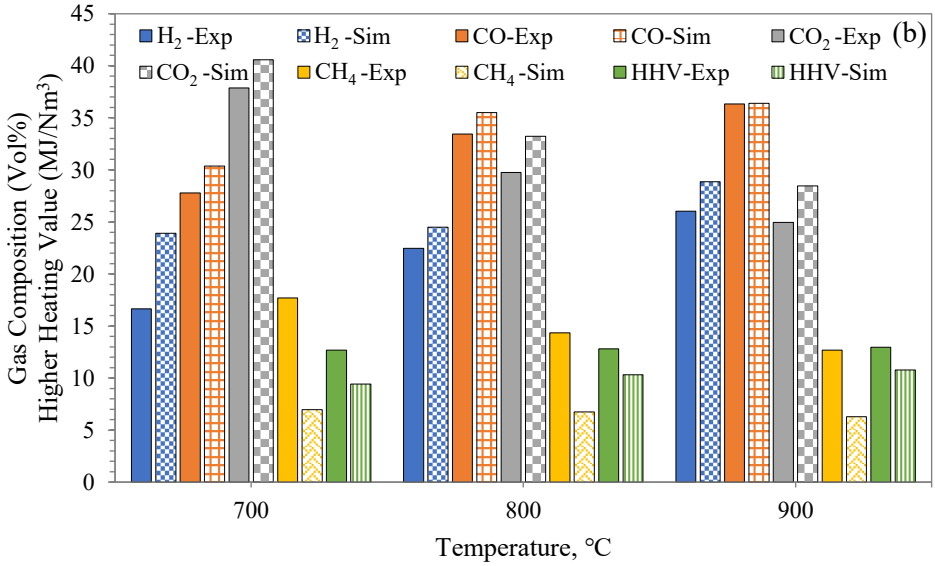

Figure 7. Impact of temperature on gas composition and syngas HHV from DPF air gasification (a) simulation results (b) validation of simulation with experimental results.

3.2.2. Impact of air flowrate on gas composition and syngas HHV

Impact of air flowrate on gas composition and syngas HHV during simulation and its validation with experimental results presented in Figure 8. Simulation results presented in Figure 8a shows that H_2, CO, and CO_2 concentrations trends are observed almost the same as the experimental results given in Figure 6a. Simulation results of methane was underestimated as compared to the experimental results for air flowrate as depicted in Figure 8b. It is mostly observed in modelling cases due to the propagations of reactions on an ideal condition [29]. At a lower air flowrate of 2 l/min H_2 and CO_2 concentration are in close agreement with experiment results. In contrast, the difference was significant in the case of CO concentration.

Whereas at the air flowrate of 3 l/min the predicted gas composition is very close to experimental gas composition. At a higher air flowrate of 4 l/min H_2 concentration, the CO and CO_2 concentration are higher in the simulation model than experimental.

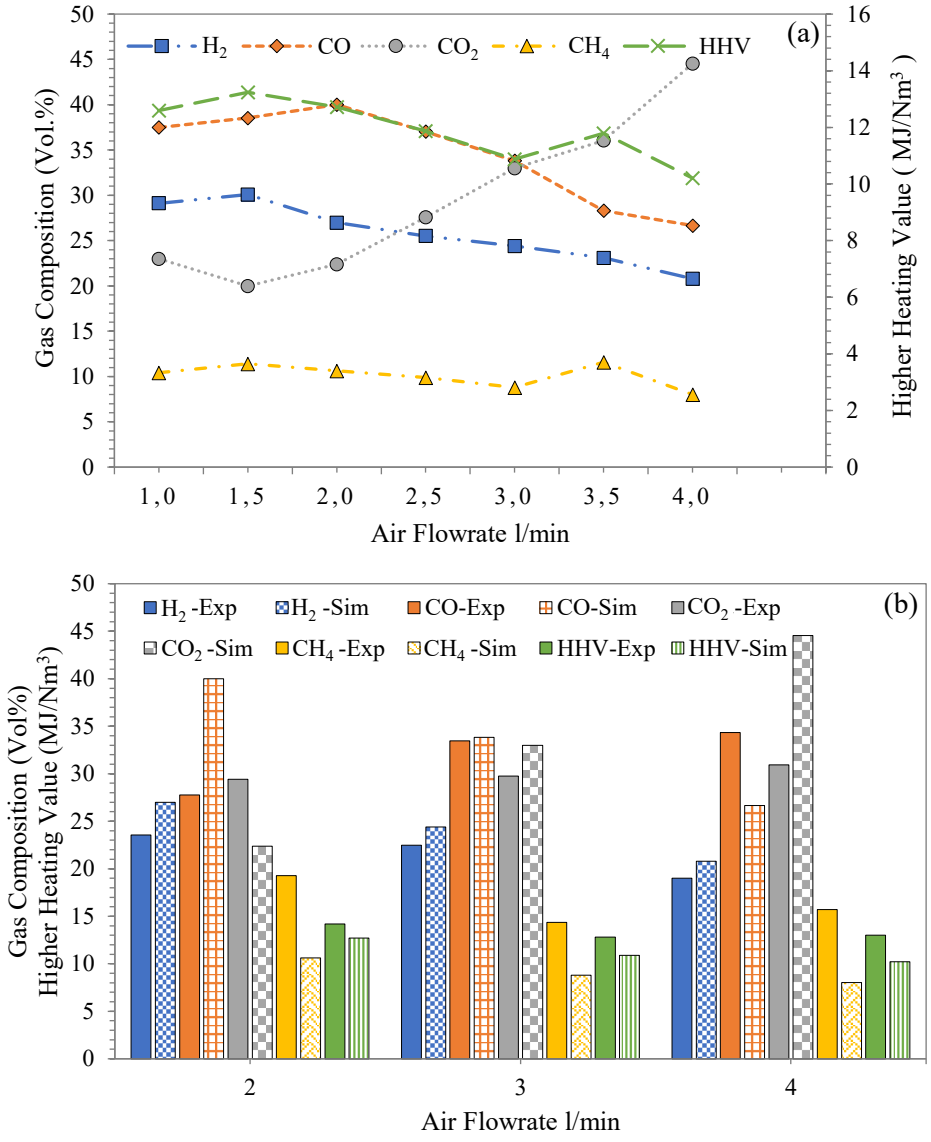

Figure 8. Impact of air flowrate on gas composition and syngas HHV from DPF air gasification (a) simulation results (b) validation of simulation with experimental results.

3.3. Mass and energy balance

The overall mass and energy flow is carried out to understand the energy required for the inputs and utilities. The heating value of product gas and energy waste in the form of ash and condensate is shown in Figure 9. Aspen plus model provides the detailed mass and energy balance. The whole system is simulated on 1000 kg of DPF at the same process conditions of the experiment. The mass and energy made at the process condition of 800°C, and air flowrate of 1500 kg/h, same as the 3 l/min of experimental condition. The DPF is fed at a temperature of 25°C carrying the 6841 MJ/h, and the air is fed at a lower temperature and has very little energy flow. Figure 9a shows an energy requirement for the heating requirement of the gasifier

is 6104.6 MJ/h to perform the gasification process. The heat requirement of a gasifier is also reported by many researchers [39,13]. Water is fed at 25℃ to cool down the gases by absorbing the heat from product gases and appears to be the most energy-carrying product is stream. The product gas consists of (H_2, CO, CO_2, CH_4, and N_2) and a total mass of 2118 kg, which carries the 7079.7 MJ/h of energy content. The product gas composition results from the endothermic reaction as the heat is supplied by heating the gasifier. The reduction of methane is due to methane reforming reaction at a higher temperature of 800℃. A very little amount of energy is carried by ash due to its significantly less formation of 30 kg. A major part of the energy associated with condensate of 13851 MJ/h is due to the absorption of heat of water from the product gas in the cooler and released in the condensate. The waste heat present in condensate in the form of hot water obtained for the cooling of product gas can be utilized within the system for the heating of reactor or other units. It can also be used for power production in an integrated system using the process heat integration concept. The future work on the utilization of this heat helps to economies the process and upscaling the process level toward commercialization.

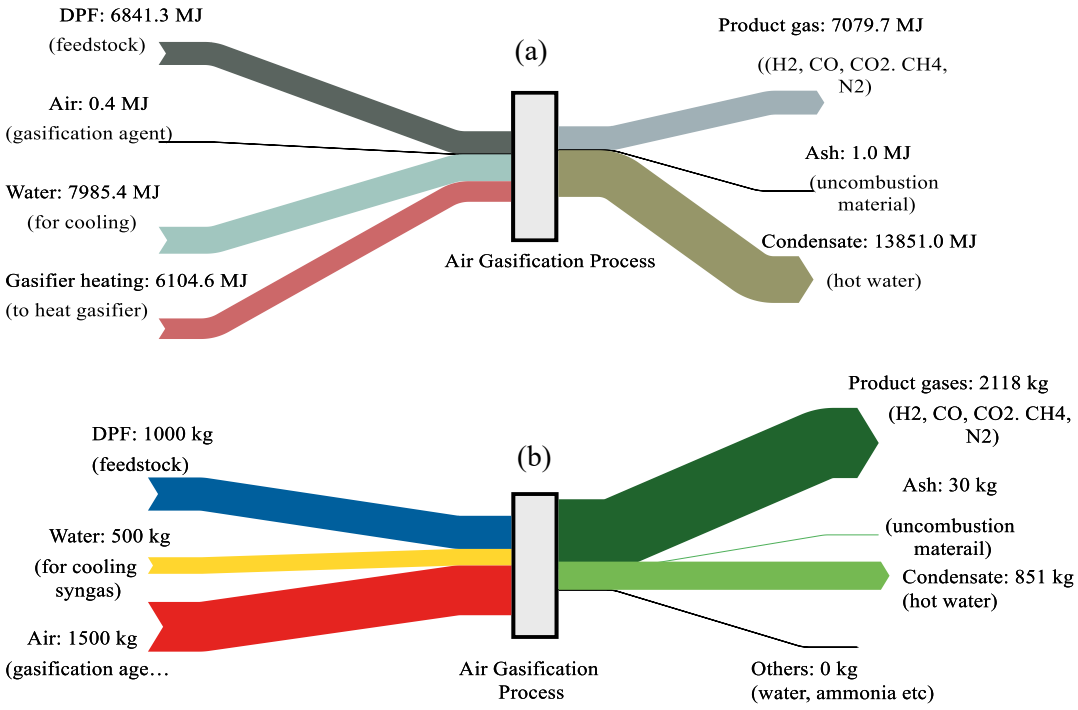

Figure 9. (a) Enthalpy balance and (b) mass for air gasification system at 800℃ temperature, particle size (d_p) 2-6 mm, and air flowrate 3 l/min.

4. Conclusions

The air gasification of DPF was instituted in fixed bed air gasification. The impact of temperature, air flowrate, and particle size on gas composition and gasification performance were investigated. In experimental results, the gas composition varies with the increase of temperature in which H_2 and CO variation about 14% and 12 vol% respectively in the forward direction. The increasing trend of H_2 and CO were also observed for increasing particle size with a small variation. In air flowrate, the maximum H_2 concentration of 28 vol% was obtained at 2.5 l/min of air flowrate and higher CO concentration at higher air flowrate. Marginally CH_4

formation decreased with the increase in temperature and air flowrate, at smaller particle size. CCE and CGE have increasing trends with the elevating temperature and particle size which was due to the increasing trend of most of gas composition. On the other hand, the air flowrate shows a different trend for the gas composition. The process simulation model predicts the gas composition is fair agreement with experimental results except for methane formation which is very low in the case of simulation. The mass and energy balance reveals that the product gas has enough heating content to generate energy and a proper heat integration needed to utilize waste heat to make the process more energy economical.

Author contribution

Mohammad R. Kabli: Conceptualization, Resources. **Arshid M. Ali:** Conceptualization, Resources, Supervision, Project administration. **Muddasser Inayat**: Conceptualization, Experimentation, Original draft writing. **Abdulrahim A. Zahrani**: Writing original draft and Editing. **Khurram Shahzad**: Writing original draft **Muhammad Shahbaz:** Writing original draft, Review & Editing, Perform statistical analysis. **Shaharin A. Sulaiman**: Conceptualization, Writing, Review & Editing.

Acknowledgements

The project was funded by the Deanship of Scientific Research (DSR) at King Abdulaziz University, Jeddah, under grant number (RG-10-135-42). The authors, therefore, acknowledge with thanks DSR technical and financial support.

Declaration of interests

☒The authors declare that they have no known competing financial interests or personal relationships that could have appeared to influence the work reported in this paper.

References

1. Liu W, Tian Y, Yan H, Zhou X, Tan Y, Yang Y, Li Z, Yuan L (2021) Gasification of biomass using oxygen-enriched air as gasification agent: a simulation study. Biomass Convers Biorefin. doi:https://link.springer.com/article/10.1007/s13399-021-02035-2

2. Shahbaz M, AlNouss A, Ghiat I, McKay G, Mackey H, Elkhalifa S, Al-Ansari T (2021) A comprehensive review of biomass based thermochemical conversion technologies integrated with CO_2 capture and utilisation within BECCS networks. Resour Conserv Recy 173:105734. doi:https://doi.org/10.1016/j.resconrec.2021.105734

3. Shahbaz M, Taqvi SAA, Inayat M, Inayat A, Sulaiman SA, McKay G, Al-Ansari T (2020) Air catalytic biomass (PKS) gasification in a fixed-bed downdraft gasifier using waste bottom ash as catalyst with NARX neural network modelling. Comput Chem Eng. 142:107048. doi:https://doi.org/10.1016/j.compchemeng.2020.107048

4. Li B, Fabrice Magoua Mbeugang C, Liu D, Zhang S, Wang S, Wang Q, Xu Z, Hu X (2020) Simulation of sorption enhanced staged gasification of biomass for hydrogen production in the presence of calcium oxide. Int J Hydrog Energ 45 (51):26855-26864. doi:https://doi.org/10.1016/j.ijhydene.2020.07.121

5. Hussain M, Zabiri H, Uddin F, Yusup S, Tufa LD (2021) Pilot-scale biomass gasification system for hydrogen production from palm kernel shell (part A): steady-state simulation. Biomass Convers Biorefin. https://doi.org/10.1007/s13399-021-01474-1

6. Wojnicka B, Ściążko M, Schmid JC (2021) Modelling of biomass gasification with steam. Biomass Conversion and Biorefinery 11 (5):1787-1805. doi:10.1007/s13399-019-00575-2

7. Suryawanshi SJ, Shewale VC, Thakare RS, Yarasu RB (2021) Parametric study of different biomass feedstocks used for gasification process of gasifier - A literature review. Biomass Convers Biorefin. https://doi.org/10.1007/s13399-021-01805-2

8. Miandad R, Barakat MA, Rehan M, Aburiazaiza AS, Ismail IMI, Nizami AS (2017) Plastic waste to liquid oil through catalytic pyrolysis using natural and synthetic zeolite catalysts. Waste Manag 69:66-78. doi:https://doi.org/10.1016/j.wasman.2017.08.032

9. Chandrasekaran M, Bahkali AH (2013) Valorization of date palm (Phoenix dactylifera) fruit processing by-products and wastes using bioprocess technology – Review. Saudi Journal of Biological Sciences 20 (2):105-120. doi:https://doi.org/10.1016/j.sjbs.2012.12.004

10. The Ministry of Environment WaA (2021) FAO approves Saudi Arabia's proposal to declare 2027 the International Year of Date Palm. https://www.mewa.gov.sa/en/MediaCenter/News/Pages/News201220.aspx. Accessed date: 28.08.202.

11. Barreveld W (1993) FAO Agricultural Services Bulletin No. 101. Food and Agriculture Organization of the United Nations

12. Amran YHA, Amran YHM, Alyousef R, Alabduljabbar H (2020) Renewable and sustainable energy production in Saudi Arabia according to Saudi Vision 2030; Current status and future prospects. J Clea Prod. 247:119602. https://doi.org/10.1016/j.jclepro.2019.119602

13. Inayat A, Shahbaz M, Khan Z, Inayat M, Mofijur M, Ahmed SF, Ghenai C, Ahmad AA (2021) Heat integration modeling of hydrogen production from date seeds via steam gasification. I J Hydrog Energ. doi:https://doi.org/10.1016/j.ijhydene.2021.02.060

14. Bensidhom G, Ben Hassen-Trabelsi A, Alper K, Sghairoun M, Zaafouri K, Trabelsi I (2018) Pyrolysis of Date palm waste in a fixed-bed reactor: Characterization of pyrolytic products. Bioresour Technol. 247:363-369. doi:https://doi.org/10.1016/j.biortech.2017.09.066

15. Sait HH, Hussain A, Salema AA, Ani FN (2012) Pyrolysis and combustion kinetics of date palm biomass using thermogravimetric analysis. Bioresour Technol. 118:382-389. doi:https://doi.org/10.1016/j.biortech.2012.04.081

16. Sait HH, Salema AA (2015) Microwave dielectric characterization of Saudi Arabian date palm biomass during pyrolysis and at industrial frequencies. Fuel 161:239-247. doi:https://doi.org/10.1016/j.fuel.2015.08.058

17. Bassyouni M, ul Hasan SW, Abdel-Aziz MH, Abdel-hamid SMS, Naveed S, Hussain A, Ani FN (2014) Date palm waste gasification in downdraft gasifier and simulation using Aspen Hyses. Energ Conver Manag 88:693-699. doi:https://doi.org/10.1016/j.enconman.2014.08.061

18. Martis R, Al-Othman A, Tawalbeh M, Alkasrawi M (2020) Energy and Economic Analysis of Date Palm Biomass Feedstock for Biofuel Production in UAE: Pyrolysis, Gasification and Fermentation. Energies 13 (22):5877. https://doi.org/10.3390/en13225877

448 19. AlNouss A, McKay G, Al-Ansari T (2018) Optimum Utilization of Biomass for the
449 Production of Power and Fuels using Gasification. In: Friedl A, Klemeš JJ, Radl S, Varbanov
450 PS, Wallek T (eds) Compu Aided Chem Eng, vol 43. Elsevier, pp 1481-1486.
451 doi:https://doi.org/10.1016/B978-0-444-64235-6.50258-8
452 20. Yaghoubi E, Xiong Q, Doranehgard MH, Yeganeh MM, Shahriari G, Bidabadi M (2018)
453 The effect of different operational parameters on hydrogen rich syngas production from
454 biomass gasification in a dual fluidized bed gasifier. Chem Eng Process Intens 126:210-221.
455 doi:https://doi.org/10.1016/j.cep.2018.03.005
456 21. Inayat M, Sulaiman SA, Kurnia JC, Shahbaz M (2019) Effect of various blended fuels on
457 syngas quality and performance in catalytic co-gasification: A review. Renew Sustain Energ
458 Rev. 105:252-267. https://doi.org/10.1016/j.rser.2019.01.059
459 22. Shahbaz M, Al-Ansari T, Inayat M, Sulaiman SA, Parthasarathy P, McKay G (2020) A
460 critical review on the influence of process parameters in catalytic co-gasification: Current
461 performance and challenges for a future prospectus. Renew Sustain Energ Rev. 134:110382.
462 doi:https://doi.org/10.1016/j.rser.2020.110382
463 23. Yusup S, Khan Z, Ahmad MM, Rashidi NA (2014). Optimization of hydrogen production
464 in in-situ catalytic adsorption (ICA) steam gasification based on Response Surface
465 Methodology. Biomass Bioenerg 60:98-107.
466 doi:https://doi.org/10.1016/j.biombioe.2013.11.007
467 24. Sulaiman SA, Naz MY, Inayat M, Shukrullah S, Ghaffar A (2019) Thermochemical
468 characteristics and gasification of date palm fronds for energy production. Theoretical
469 Foundations of Chemical Engineering 53 (6):1083-1093.
470 https://doi.org/10.1134/S0040579519060113
471 25. Taba EL, Irfan MF, Wan Daud WAM, Chakrabarti MH (2012) The effect of temperature
472 on various parameters in coal, biomass and CO-gasification: A review. Renew Sustain Energ
473 Rev 16 (8):5584-5596. doi:http://dx.doi.org/10.1016/j.rser.2012.06.015
474 26. Lahijani P, Zainal ZA (2011) Gasification of palm empty fruit bunch in a bubbling fluidized
475 bed: A performance and agglomeration study. Bioresour Technol 102 (2):2068-2076.
476 doi:http://doi.org/10.1016/j.biortech.2010.09.101
477 27. Taba EL, Irfan MF, Wan Daud WMA, Chakrabarti MH (2013) Fuel blending effects on
478 the co-gasification of coal and biomass - A review. Biomass Bioenerg 57 (0):249-263.
479 doi:http://dx.doi.org/10.1016/j.biombioe.2013.02.043
480 28. Xiao R, Zhang M, Jin B, Huang Y (2006) High-temperature air/steam-blown gasification
481 of coal in a pressurized spout-fluid bed. Energ Fuel. 20 (2):715-720.
482 https://doi.org/10.1021/ef050233h
483 29. Shahbaz M, Yusup S, Inayat A, Ammar M, Patrick DO, Pratama A, Naqvi SR (2017)
484 Syngas production from steam gasification of palm kernel shell with subsequent CO_2 capture
485 using CaO sorbent: an Aspen Plus modeling. Energ Fuel 31 (11):12350-12357.
486 https://doi.org/10.1021/acs.energyfuels.7b02670
487 30. González AM, Lora EES, Palacio JCE, del Olmo OAA (2018) Hydrogen production from
488 oil sludge gasification/biomass mixtures and potential use in hydrotreatment processes. Int J
489 Hydrog Energ 43 (16):7808-7822. https://doi.org/10.1016/j.ijhydene.2018.03.025

490 31. Lapuerta M, Hernández JJ, Pazo A, López J (2008) Gasification and co-gasification of
491 biomass wastes: Effect of the biomass origin and the gasifier operating conditions. Fuel Process
492 Technol 89 (9):828-837. doi:http://doi.org/10.1016/j.fuproc.2008.02.001
493 32. Mahishi MR, Goswami DY (2007) An experimental study of hydrogen production by
494 gasification of biomass in the presence of a sorbent. Int J Hydrog Energ 32 (14):2803-2808.
495 doi:http://doi.org/10.1016/j.ijhydene.2007.03.030
496 33. Ahmad AA, Zawawi NA, Kasim FH, Inayat A, Khasri A (2016) Assessing the gasification
497 performance of biomass: A review on biomass gasification process conditions, optimization
498 and economic evaluation. Renew Sustain Energ Rev 53:1333-1347.
499 https://doi.org/10.1016/j.rser.2015.09.030
500 34. Ul Hai I, Sher F, Yaqoob A, Liu H (2019) Assessment of biomass energy potential for SRC
501 willow woodchips in a pilot scale bubbling fluidized bed gasifier. Fuel 258:116143.
502 doi:https://doi.org/10.1016/j.fuel.2019.116143
503 35. Gálvez-Pérez A, Martín-Lara MA, Calero M, Pérez A, Canu P, Blázquez G (2021)
504 Experimental investigation on the air gasification of olive cake at low temperatures. Fuel
505 Process Technol 213:106703. doi:https://doi.org/10.1016/j.fuproc.2020.106703
506 36. Inayat M, Sulaiman SA, Kumar A, Guangul FM (2016) Effect of fuel particle size and
507 blending ratio on syngas production and performance of co-gasification. J Mech Eng Sci. 10
508 (2):2187-2199. doi:https://doi.org/10.15282/jmes.10.2.2016.21.0205
509 37. Kirubakaran V, Sivaramakrishnan V, Nalini R, Sekar T, Premalatha M, Subramanian P
510 (2009) A review on gasification of biomass. Rennew Sustain Energ Rev 13 (1):179-186.
511 doi:http://dx.doi.org/10.1016/j.rser.2007.07.001
512 38. Fremaux S, Beheshti S-M, Ghassemi H, Shahsavan-Markadeh R (2015) An experimental
513 study on hydrogen-rich gas production via steam gasification of biomass in a research-scale
514 fluidized bed. Energ Convers Manag 91:427-432.
515 doi:https://doi.org/10.1016/j.enconman.2014.12.048
516 39. Khan Z, Yusup S, Kamble P, Naqvi M, Watson I (2018) Assessment of energy flows and
517 energy efficiencies in integrated catalytic adsorption steam gasification for hydrogen
518 production. Appl Energ 225:346-355. https://doi.org/10.1016/j.apenergy.2018.05.020
519